Dynamical thermal response functions for strongly correlated one-dimensional systems: Hubbard and spinless fermion *t*-*V* model

Michael R. Peterson,[1,*] Subroto Mukerjee,[2,3] B. Sriram Shastry,[1] and Jan O. Haerter[1]
[1]*Physics Department, University of California, Santa Cruz, California 95064, USA*
[2]*Department of Physics, University of California, Berkeley, California 94720, USA*
[3]*Materials Sciences Division, Lawrence Berkeley National Laboratory, Berkeley, California 94720, USA*
(Received 7 June 2007; published 20 September 2007)

In this paper, we study the thermal response functions for two one-dimensional models, namely, the Hubbard and spinless fermion *t*-*V* model, respectively. By exactly diagonalizing finite sized systems, we calculate dynamical, electrical, thermoelectrical, and thermal conductivities via the Kubo formalism [J. Phys. Soc. Jpn. **12**, 570 (1957)]. The thermopower (Seebeck coefficient), Lorenz number, and dimensionless figure of merit are then constructed, which are quantities of great interest to the physics community both theoretically and experimentally. We also geometrically frustrate these systems and destroy integrability by the inclusion of a second-neighbor hop in the kinetic energy operator. These frustrated systems are shown to have enhanced thermopower and Lorenz number at intermediate and low temperatures.

DOI: 10.1103/PhysRevB.76.125110 PACS number(s): 72.15.Jf, 65.90.+i, 71.27.+a, 71.10.Fd

I. INTRODUCTION

Strongly correlated electron systems are currently at the forefront of physics providing some of the most interesting theoretical challenges and many experimental systems of fundamental and technological interest.[1,2] It is at the convergence of the fundamental and the technological that thermal response functions of strongly correlated systems take on particular importance. This is certainly true in the high thermopower material sodium cobalt oxide[3–6] as well as other transition metal oxides such as the high T_c superconductors. Furthermore, thermal behavior is also important in experimental one-dimensional systems such as carbon nanotubes,[7] semiconductor nanowires,[8] and organic compounds,[9,10] to name a few.

In addition to strong electron correlations, frustration[11] has generated much interest in the physics community throughout the past decades. Recently, it has been shown that strong electron correlations in conjunction with the electronic frustration introduced by a two-dimensional triangular lattice are the keys to understanding the Curie-Weiss metallic phase in sodium cobalt oxide.[6] Frustration is also the key to the emergence of kinetic antiferromagnetism[12] and to a description of quantum spin glasses.[11]

In this paper, we concentrate on the electrical and thermal transport of one-dimensional systems which often display exotic collective behavior due to the reduced dimensionality, most strikingly exemplified in the Luttinger liquid at low temperatures.[13] One dimension also allows the existence of a class of systems known as integrable systems, where there exists an infinite family of mutually commuting operators that commute with the Hamiltonian.[14–16]

Frustration can be introduced into a one-dimensional system by considering kinetic energy hoppings further than nearest neighbors, i.e., second nearest neighbors. In this work, we demonstrate that electronic frustration of this sort also has very interesting effects on transport properties in addition to the equilibrium properties alluded to above. One such effect, recently predicted by Shastry and co-workers,[6,17–19] is the enhancement of the thermopower compared to the unfrustrated system. This enhancement arises from electron transport on general grounds related to electronic frustration; however, a quantitative measure is only possible by computations such as those described in this paper. Clearly, this thermopower enhancement is potentially of great interest to the material science community since it provides clues in the search for large thermopower materials.

Theoretically, strongly correlated systems are notoriously difficult to study due in part to the failure and/or tenuous applicability of perturbation theory. The exact calculation of dynamical thermal response functions (using the Kubo[20] formalism) requires knowledge of the full eigenspectrum and, therefore, progress is made via exact diagonalization of finite sized systems. Furthermore, recently Shastry[17–19] has introduced a new high frequency formalism for thermoelectrics (discussed below) that is particularly suited for strongly correlated electron systems by essentially disentangling the interactions from the dynamics and one-dimensional systems provide a good playground in which to gauge and explore this new high frequency formalism.

The models and systems we study are prototypical strongly correlated one-dimensional models, namely, the Hubbard and spinless fermion *t*-*V* model, respectively. In this work, we consider rings (periodic boundary conditions) of up to $\mathcal{L}=10$ sites for the Hubbard model and $\mathcal{L}=16$ sites for the spinless fermion *t*-*V* model. Of course, newer approximate theoretical methods, in lieu of exact diagonalization, are constantly being developed, such as the dynamical mean field theory,[21,22] finite temperature Lanczos (FTL) method,[23] cluster perturbation theory,[24] etc. In fact, the dynamical mean field theory approximation has considered some thermoelectric variables for the one-dimensional Hubbard model previously, although in a limited range of model parameter space (see Refs. 25 and 26). However, an important first step is to approach these systems with a rigorously exact method (exact diagonalization) to, if nothing else, provide a benchmark for further approximate studies and methods.

There are, however, obvious shortcomings to exact diagonalization, i.e., finite size effects due to the smallness of the

system and the computational price paid is often expensive. That being said, we find only the very low temperature regimes ($T<1|t|$) troublesome in our studies which, incidentally, are the regimes that other approximations also have difficulty tackling. These difficulties are expected on general grounds for any finite system study since the mean energy level spacing becomes comparable to the thermal energy. Experimentally, often the most interesting case corresponds to intermediate temperatures, where we do much better. Furthermore, the high frequency formalism of Shastry is significantly less expensive computationally and could lend itself more profitably to new and existing approximate methods.

We primarily use the Hubbard model for our studies and carry out the most extensive calculations on it, while the t-V model is mainly supplemental.[27] The thermopower is the most tractable observable calculated and is, therefore, considered more extensively. We emphasize that the computations presented here for the thermopower, Lorenz number, and dimensionless figure of merit for these strongly correlated models consider the full range of model parameter space.

The plan of this paper is as follows: In Sec. II, we introduce the models to be studied and provide an overview of our exact diagonalization procedure. Section III reviews the Kubo formalism for the thermoelectric conductivities needed to calculate the physical observables of interest as well as briefly describes the high frequency formalism of Shastry. In Sec. IV, we study the thermopower for the Hubbard and t-V models for the unfrustrated and frustrated cases explicitly demonstrating thermopower enhancement for the frustrated systems. Sections V and VI present results for the Lorenz number and thermoelectric figure of merit (FOM) for the Hubbard model, again for the unfrustrated and frustrated cases. Conclusions are presented in Sec. VII.

II. HUBBARD AND t-V MODELS

Here, we describe in detail the considered models, namely, the unfrustrated (frustrated) Hubbard and t-V models with a second-nearest-neighbor hopping amplitude $t'=0$ ($t' \neq 0$). In the frustrated scenario, an electron can hop back to its original starting place in three hops with a hopping amplitude $(-t)^2 t' = t^2 t'$. When $t'<0$, the system is electronically frustrated and this, as will be shown, leads to an enhanced thermopower and Lorenz number.

The Hubbard model is described by a Hamiltonian with a kinetic energy term allowing electron hopping between sites j and $j+\eta$ with probability $t(\eta)$ and an on-site electron repulsion potential energy governed by parameter U, i.e.,

$$\hat{H} = -\sum_{j=1}^{\mathcal{L}} \sum_{\eta=1}^{2} \sum_{\sigma} t(\eta)\{\hat{c}^{\dagger}_{j+\eta\sigma}\hat{c}_{j\sigma} + \text{H.c.}\} + U\sum_{j=1}^{\mathcal{L}} (\hat{n}_{j\uparrow} - 1/2)(\hat{n}_{j\downarrow} - 1/2), \tag{1}$$

where $\hat{c}^{\dagger}_{j\sigma}$ ($\hat{c}_{j\sigma}$) creates (destroys) an electron with spin $\sigma = (\uparrow, \downarrow)$ at the lattice site j, $\hat{n}_{j\sigma} = \hat{c}^{\dagger}_{j\sigma}\hat{c}_{j\sigma}$ is the number operator, and $\eta=1$ and $\eta=2$ for first and second nearest neighbor hoppings, respectively. The electron operators obey the usual anticommutation rules $\{\hat{c}_{j\sigma}, \hat{c}^{\dagger}_{j'\sigma'}\} = \delta_{jj'}\delta_{\sigma\sigma'}$. We assume $t(1) = t$, $t(2) = t'$, and $t(\eta) = 0$ for all other η. With $t'=0$, this unfrustrated Hamiltonian is particle-hole symmetric as can be seen from the local transformation $\hat{d}^{\dagger}_{j\sigma} = (-1)^j \hat{c}_{j\sigma}$. This transformation leaves t and U invariant, while taking $N_\sigma \to \mathcal{L} - N_\sigma$, where N_σ is the total number of electrons with spin σ and the total number of electrons is $N = \Sigma_\sigma N_\sigma$. The frustrated case ($t' \neq 0$) breaks particle-hole symmetry since it takes $t' \to -t'$. However, even for the frustrated case, the above transformation is useful since it informs us that a quantity $A(N_\uparrow, N_\downarrow, t, t', U) = \pm A(\mathcal{L} - N_\uparrow, \mathcal{L} - N_\downarrow, t, -t', U)$. Knowing the value of A up to half-filling for t' and $-t'$ allows us to construct the entire dependence on filling in both cases (unfrustrated and frustrated), provided we know the parity of A under the particle-hole transformation. We only consider electron repulsion $U>0$ and assume periodic boundary conditions (one-dimensional rings).

The spinless fermion t-V model is governed by a Hamiltonian with a kinetic energy term similar to the Hubbard model (without the spin) and a potential energy describing a nearest-neighbor repulsion governed by a parameter V, i.e.,

$$\hat{H} = -\sum_{j=1}^{\mathcal{L}} \sum_{\eta=1}^{2} t(\eta)\{\hat{c}^{\dagger}_{j+\eta}\hat{c}_j + \text{H.c.}\} + V\sum_{j=1}^{\mathcal{L}} (\hat{n}_j - 1/2)(\hat{n}_{j+1} - 1/2). \tag{2}$$

Again, we assume here that $t(1)=t$, $t(2)=t'$, and $t(\eta)=0$ for all other η and $V>0$. This model too has the same particle-hole symmetry but without the spin. It is clear that t' breaks the particle-hole symmetry and a calculation up to half-filling (with $t'>0$ and $t'<0$) suffices, allowing extrapolation to all fillings.

As with any exact diagonalization procedure, there exist computational limitations due to the obvious difficulties in dealing with large matrices. In view of these limitations,[28] the Hubbard model is computed for $N=1,\ldots,5$ and 5,…,8 electrons on $\mathcal{L}=10$ and 8 site systems, respectively. These particular systems correspond to electron fillings (densities) of $n=N/\mathcal{L}=0.1$, 0.2, 0.3, 0.4, 0.5, 0.625, 0.75, 0.875, and 1. The t-V model allows a larger cluster size stemming from the lack of the spin degree of freedom (smaller comparative Hilbert space) and we present results for $L=16$ and $N=1,\ldots,8$. The large Hilbert spaces can be reduced by considering systems with a constant z component of spin (for the Hubbard model). The sector with the smallest z component of spin has the largest Hilbert subspace dimension and dominates the physics. Linear momentum is a good quantum number due to the translational invariance of our systems and we implement this symmetry to further reduce the Hilbert space to more manageable proportions. However, we point out that the bottleneck of our calculations is not necessarily the Hamiltonian diagonalization but the finite temperature averages of certain operators and the evaluation of the full Kubo formulas discussed below.

It is well known that density of states of our models for $t'=0$ has two Van Hove singularities at the band edges. If $|t'|>0.25|t|$, another singularity is introduced, which will in-

variably produce large changes in the thermoelectric properties. However, we are interested here in the more subtle effects arising from geometrical frustration and strong interactions. Hence, by introducing a nonzero $|t'|<0.25|t|$, the density of states maintains only the original two van Hove singularities. Another motivating factor for choosing $|t'|<0.25|t|$ is that it is known[29] that for $|t'|\geqslant 0.5|t|$, a rich ground state phase diagram is seen for half-filling in the frustrated one-dimensional Hubbard model. While interesting in itself, this would serve to unnecessarily complicate our present analysis.

In order to display effects of electron correlations, the interaction parameter $U(V)$ must be at least a few times larger than the bandwidth which is equal to $W=4|t|$ for both models. We consider three values of interaction strength for each model corresponding roughly to the noninteracting case where the interaction parameter is equal to zero $[U(V)=0 \ll W]$, the weakly interacting case where the interaction is equal to roughly the bandwidth $[U(V)\sim W]$, and the strongly interacting case where the interaction is a few times greater than the bandwidth $[U(V)\gg W]$.

III. DYNAMICAL THERMAL RESPONSE FUNCTIONS AND SHASTRY'S HIGH FREQUENCY FORMALISM

Conductivities are computed via the Kubo linear response formalism[30] recently presented in detail by Peterson *et al.* in Ref. 31 which closely followed the work of Shastry.[17–19] In particular, we calculate the Kubo formulas for the electrical $\sigma(\omega)$, thermoelectrical $\gamma(\omega)$, and the thermal $\kappa(\omega)$ conductivities, respectively, which then allows us to calculate physical quantities of interest such as the thermopower S (or Seebeck coefficient) (the ratio of the thermoelectrical to electrical conductivities), the Lorenz number L (the ratio of the thermal conductivity to the electrical conductivity divided by T under zero current conditions), and the dimensionless figure of merit ZT, given as

$$S(\omega,T)=\frac{\gamma(\omega,T)}{\sigma(\omega,T)}, \tag{3}$$

$$L(\omega,T)=\frac{\kappa(\omega,T)}{T\sigma(\omega,T)}-S(\omega,T)^2, \tag{4}$$

and

$$Z(\omega,T)T=\frac{S(\omega,T)^2}{L(\omega,T)}. \tag{5}$$

The second term in Eq. (4) is produced by the zero electric current constraint under a thermal gradient.[32] This term is usually small (especially at low temperatures) for metals and semiconductors and often ignored. However, as will be shown, for strongly correlated lattice systems like those studied here, this term is an important factor especially at high temperatures.

One is usually interested in the dc $(\omega\to 0)$ limit of the dynamical conductivities. For finite sized systems, this requires the introduction of a level broadening ϵ which smoothens the divergences caused by the discrete nature of the eigenspectrum. Often, ϵ is taken to be equal to the mean energy level spacing of the system which is of order $\mathcal{O}(|t|/\mathcal{L})$. However, for the Hubbard model, as the interaction energy U is increased, the mean energy level spacing begins to include upper Hubbard bands. In Figs. 1(a)–1(c), the probability density of states $P(s)$ with energy difference $s=|\varepsilon_i-\varepsilon_j|$ (ε_k is the eigenenergy of state k) is plotted for three representative cases, namely, fillings $n=0.3$, 0.5, and 0.9, for $U=4|t|$ (weakly coupled) and $U=12|t|$ (strongly coupled). It is clear in Figs. 1(a)–1(c) that the most probable energy difference between states in the lower Hubbard band is relatively immune to changes in either filling or interaction strength. However, the appearance of the upper Hubbard bands in the strongly coupled case yields an ϵ that is very large (compared to the bandwidth) and strongly U dependent. This large ϵ tends to mask real physical contributions to the current matrix elements coming from transitions within the lower Hubbard band at the expense of broadening transitions between Hubbard bands. Therefore, in this work, we choose ϵ to be approximately equal to the mean energy level spacing in the lower Hubbard band for all cases, i.e., $\epsilon=0.8|t|$ for the Hubbard model.[33]

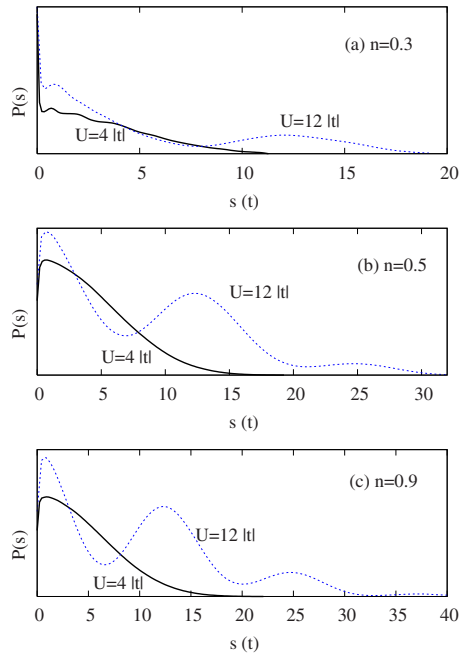

FIG. 1. (Color online) Probability density of states $P(s)$ with energy difference $s=|\varepsilon_i-\varepsilon_j|$. The solid black and dashed blue (black) lines represent $U=4|t|$ and $12|t|$, respectively, for density (a) $n=0.3$, (b) $n=0.5$, and (c) $n=0.9$. The position of the maximum probability for the lower Hubbard band is insensitive to the value of U.

As discussed previously in detail in Ref. 31, another frequency limit (besides the dc limit) is the infinite frequency limit, defined for the thermopower, Lorenz number, and figure of merit as

$$S^*(T)=\lim_{\omega\to\infty} S(\omega,T)=\frac{\langle\hat{\Phi}_{xx}\rangle}{T\langle\hat{\tau}_{xx}\rangle}, \tag{6}$$

$$L^*(T) = \lim_{\omega\to\infty} L(\omega,T) = \frac{\langle\hat{\Theta}_{xx}\rangle}{T^2\langle\hat{\tau}_{xx}\rangle} - [S^*(T)]^2, \tag{7}$$

and

$$Z^*(T)T = \lim_{\omega\to\infty} Z(\omega,T)T = \frac{[S^*(T)]^2}{L^*(T)}, \tag{8}$$

respectively, with the operators $\hat{\tau}_{xx}$, $\hat{\Phi}_{xx}$, and $\hat{\Theta}_{xx}$ defined in Refs. 17–19. The benefit of such a limit is that these quantities can be calculated as equilibrium expectation values of operators that, while nontrivial, are easier to calculate and less time consuming numerically than the full dynamical quantities via the Kubo formulas. All of the interaction effects remain in these quantities but, importantly, the dynamics has been separated from the interactions. A further ambition of this work is to determine the evolution of the considered physical observables as functions of frequency, temperature, and density from the dc to the infinite frequency limit allowing a complete picture of the accuracy and/or limitations of the infinite frequency formalism of Shastry.

IV. THERMOPOWER

The thermopower, being the ratio of the thermoelectrical to the electrical conductivity, measures the electrical response of a material to a temperature gradient. Like the Hall coefficient, it is often assumed to measure the sign of the charge carriers in a particular material.

The thermopower $S(\omega,T)$ can be instructively rewritten,[6,31] by isolating the term containing the chemical potential $\mu(T)$, as

$$S(\omega,T) = S_{tr}(\omega,T) + S_{MH}(T). \tag{9}$$

The first term is due to electrical transport, while the second is entropic in origin and is the familiar Mott-Heikes[34] term $S_{MH}(T) = -[\mu(T) - \mu(0)]/q_eT$. These two terms both contribute to the thermopower in different and often competing ways.

In strongly correlated systems, the first term in Eq. (9) is usually the most intractable. For many systems, this term is small (especially at low temperatures) compared to the second term and is fruitfully ignored. In this approximation, the thermopower is dominated by the Mott-Heikes (MH) term. The MH limit is described as the limit when $k_BT \gg |t|$. This limit is achieved either at very high temperatures or at more modest temperatures in narrow band systems.[34] The usefulness of the MH term is that at high temperatures, the chemical potential is linear in T, leaving the MH limit constant in temperature but with a nontrivial filling dependence arising from the particular nature of the Hilbert space. Many of these MH limits were considered previously[34] and below we quote them for the spinless fermion t-V model for finite and infinite V in Eq. (11). As will be shown below, the transport term [first term in Eq. (9)] is very important for low to intermediate temperatures and using MH term alone for the thermopower is clearly inadequate.

The thermopower is expected to vanish in the zero temperature limit. This is physically intuitive and has been shown theoretically for the one-dimensional Hubbard model via a version of the Bethe ansatz solution.[35] In our formalism, this vanishing is accomplished through a subtle balance of the transport and MH terms as $T\to 0$, and for thermodynamically large systems, this balance is obtained. However, for finite systems, even in the noninteracting limit, the balance is not manifest, resulting in thermopower divergences as $T\to 0$ due to finite size effects. However, this suggests a rewriting of the thermopower, given in Refs. 6 and 31, in such a way to ensure that the thermopower vanishes at $T=0$ by forcing both the transport $[(S_{tr}(\omega,T))]$ and MH $[(S_{MH}(T))]$ terms to independently vanish as $T\to 0$. This rewriting yields a frequency dependent transport term and a frequency independent MH term.

Finite sized systems have a few more subtleties which we now describe. The chemical potential is commonly defined as $\mu(T) = \partial F_N(T)/\partial N$, where $F_N(T)$ is the Helmholtz free energy for an N particle system. For our finite systems, we will approximate this partial derivative as $\mu(T) = [F_{N+1}(T) - F_{N-1}(T)]/2$ for $N \geqslant 2$ and necessarily $\mu(T) = F_{N+1}(T) - F_N(T)$ for $N=1$. As discussed in Ref. 31, the ground state degeneracy of a system (if it exists) is discounted when calculating $\mu(T)$ so as to eliminate a leading order term linear in T that produces a nonzero $S_{MH}(T)$ as $T\to 0$. Further, finite systems have discrete energy levels giving rise to an energy gap. The energy gap causes an exponential behavior in $\mu(T)$ which is not a serious problem since it vanishes faster than T^2. Both of these particulars, however, create a chemical potential which does not behave as T^2 at low T as expected for thermodynamically large systems.

In the following figures, the thermopower will be given in its "natural" units of k_B/q_e, where $q_e = -|e|$ with $|e|$ the value of the electron charge. For experimental comparison, one simply replaces $k_B/|e| = 86\ \mu\text{V/K}$.

A. Hubbard model

The MH term is the high temperature limit $k_BT \gg |t|$ of $S_{MH}(T)$. As discussed elsewhere,[31,34] the MH limit of the finite U situation is essentially the uncorrelated band since the temperature is necessarily much larger than U. To understand the effects strong interactions play (large U), one must consider infinite U when calculating this limit.

In the finite U case, the MH limit has a single zero crossing at half-filling $n=1$ where the thermopower is seen to change sign and it diverges in the band-insulator limits ($n=0$ and $n=2$). For the infinite U, case there are two additional zero crossings and one additional divergence. The MH limit still diverges in the band-insulator limits but now also diverges for the Mott insulator ($n=1$). The two additional sign changes occur for fillings $n=2/3$ and $n=4/3$. The MH limit in the infinite U case for $n \geqslant 1$ is found from the MH limit for $0 \geqslant n \geqslant 1$ through particle-hole symmetry ($n\to 2-n$ and $q_e\to -q_e$). There is no t' dependence for the MH limits; therefore, they lead to the conclusion (for t and t') that the Hubbard model should have interaction induced sign changes of the thermopower at $n \approx 2/3$ (and $n \approx 4/3$ using particle-hole symmetry).

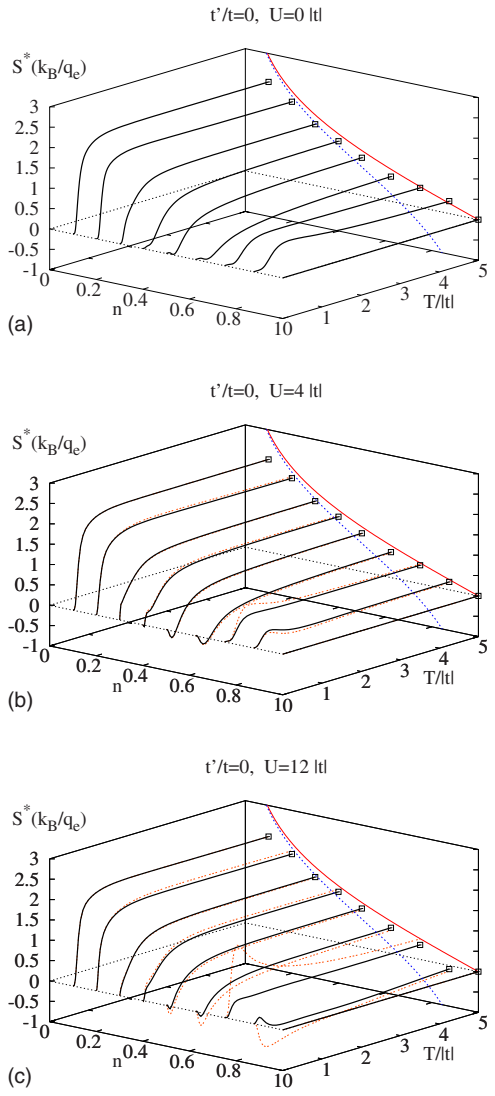

FIG. 2. (Color online) $S^*(T)$ (black line) as a function of filling n and temperature T. For (b) and (c), the orange (gray) dotted lines are the dc limit $S(0,T)$ of the full thermopower for comparison. Projected onto the $T=5|t|$ plane are the MH limits for both the finite [red (gray) line] and infinite U [blue (black) dashed line] situations.

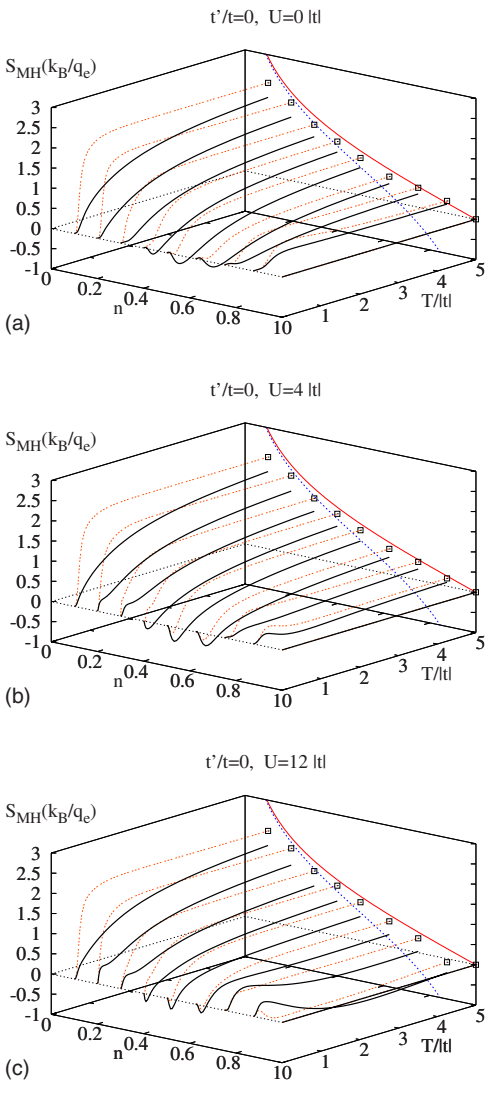

FIG. 3. (Color online) $S_{MH}(T)$ (black line) as a function of filling n and temperature T. For (b) and (c), the orange (gray) dotted lines are the infinite frequency limit $S^*(T)$ for comparison. Projected onto the $T=5|t|$ plane are the MH limits for both the finite [red (gray) line] and infinite U [blue (black) dotted line] cases.

First, we consider results for the unfrustrated Hubbard model ($t'=0$).

1. Unfrustrated thermopower (Hubbard)

Here, we consider the Hubbard model with $t'=0$ in the noninteracting ($U=0$), the weakly correlated ($U=4|t|$), and the strongly correlated ($U=12|t|$) cases, respectively.

Due to the particle-hole symmetry of the $t'=0$ Hubbard model, $\mu(T)$ for $N=\mathcal{L}$ is

$$\mu(T) = \frac{1}{2\beta}\ln\left(\frac{\mathcal{Z}_{\mathcal{L}-1}}{\mathcal{Z}_{\mathcal{L}+1}}\right) = \frac{1}{2\beta}\ln\left(\frac{\mathcal{Z}_{\mathcal{L}-1}}{e^{-\beta U}\mathcal{Z}_{\mathcal{L}-1}}\right) = \frac{U}{2}, \quad (10)$$

since an energy eigenstate for N electrons and for $2\mathcal{L}-N$ electrons are related through $\varepsilon_k(N)=\varepsilon_k(2\mathcal{L}-N)-(\mathcal{L}-N)U$ according to Lieb and Wu.[36] Hence, $S_{MH}(T)$ is identically zero for all T. The transport term $S_{tr}(T)$ is also identically zero for all T due to particle-hole symmetry and hence we find that $S(\omega,T)=0$ for $n=1$ for all T and ω. This argument equally applies to the spinless t-V model for $t'=0$.

In Figs. 2(a)–2(c), we plot the infinite frequency limit of the thermopower $S^*(T)$ and the dc limit ($\omega\to 0$) of the full Kubo thermopower $S(\omega,T)$ versus temperature T and filling n for $U=0|t|$ (a), $4|t|$ (b), and $12|t|$ (c). Projected onto the $T=5|t|$ plane are the MH limits for finite and infinite U scenarios.

For the noninteracting case in Fig. 2(a), there is no frequency dependence as both the charge and heat current operators are diagonal. The thermopower grows monotonically and, essentially, linearly from zero at $T=0$ to the MH limit[37] near $T=5|t|$. As the temperature is increased, the slope of the linear regime is lessened and the thermopower approaches the MH limit more slowly. Some finite size effects are evi-

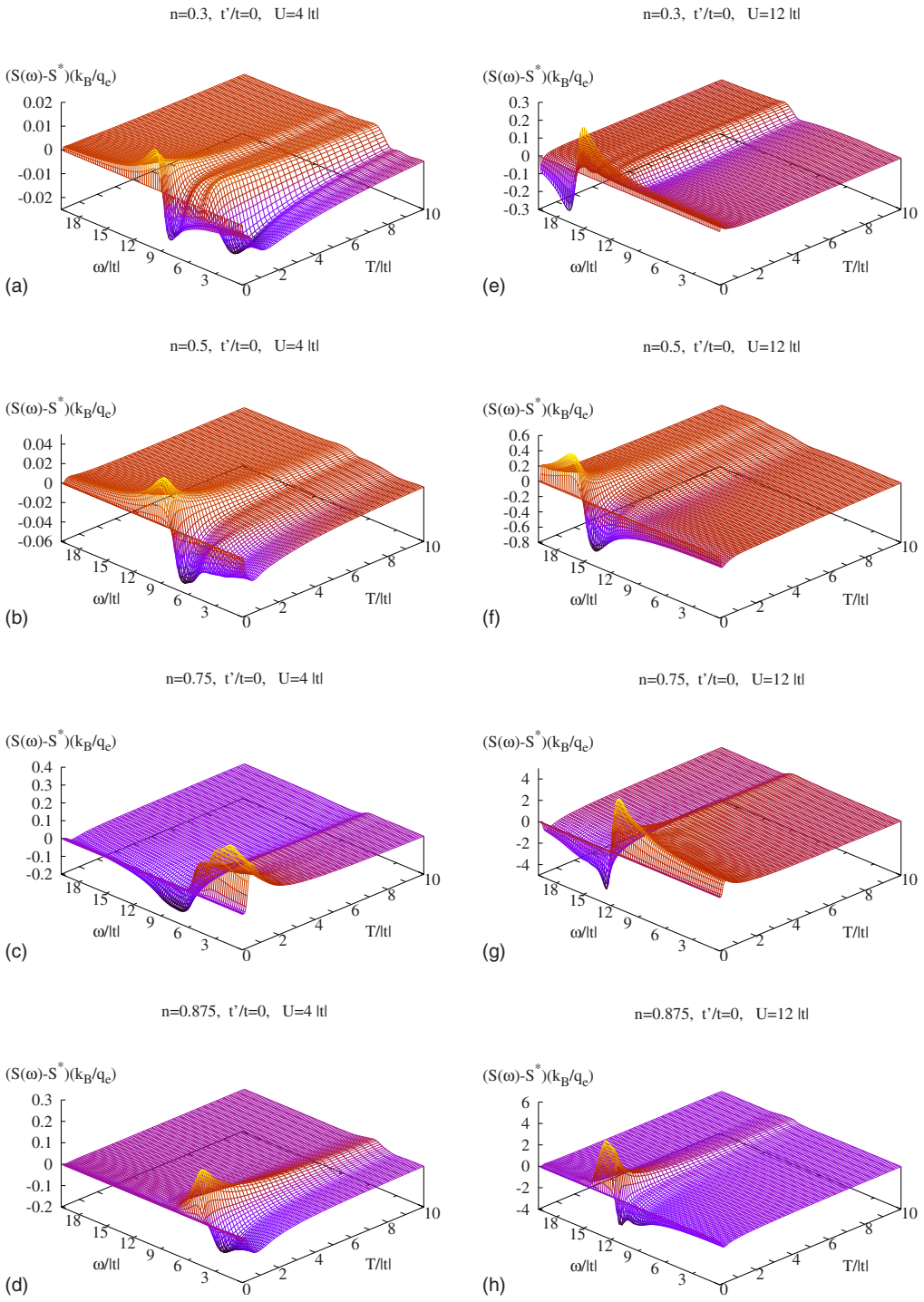

FIG. 4. (Color online) $S(\omega,T)-S^*(T)$ as a function of frequency ω and temperature T for the weak coupling case $U=4|t|$, $t'=0$, and fillings (a) $n=0.3$, (b) $n=0.5$, (c) $n=0.75$, and (d) $n=0.875$. Panels (e)–(h) represent the strong coupling case $U=12|t|$ for fillings the same as those for the weak coupling case. The main frequency dependence occurs near $\omega \sim U$ for low to intermediate temperatures. The largest frequency dependence near $T=0$ is likely a finite size effect. There is no frequency dependence for the half-filled case $n=1$ (not shown).

dent at the largest fillings $n=6/8$ and $7/8$ calculated where some somewhat strange low temperature effects are observed.

The effect of interactions shown in Figs. 2(b) and 2(c) is to generally reduce the thermopower for fillings greater than $n=2/3$. For fillings below $n \sim 0.625$, the dc and infinite frequency thermopower are essentially identical. At fillings greater than $n=0.625$, $S(0,T)$ and $S^*(T)$ display slight differences at low temperatures for the weakly correlated regime [$U=4|t|$, Fig. 2(b)] and marked differences for the strongly interacting regime [$U=12|t|$, Fig. 2(c)].

The thermopower at half-filling in all cases is pinned at zero as discussed. For $n=0.875$, the effect of interactions is to reduce the thermopower [Fig. 2(b)], changing its sign

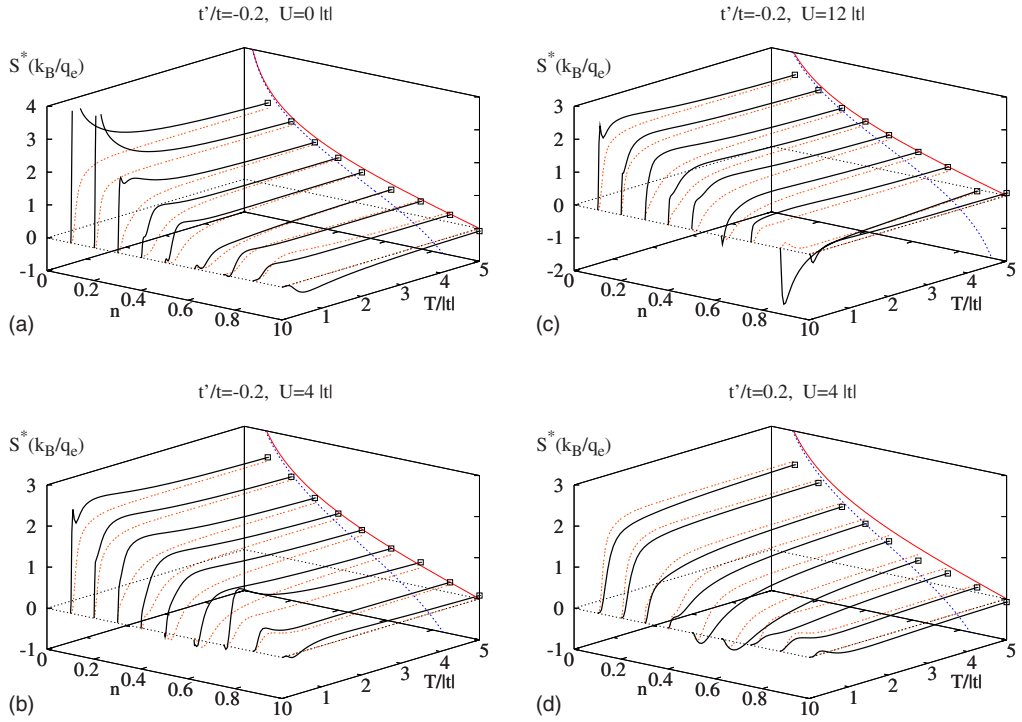

FIG. 5. (Color online) $S^*(T)$ (black line) as a function of filling n and temperature T for (a) $U=0$, (b) $U=4|t|$, and (c) $U=12|t|$ and $t'/t=-02$. The full $S(\omega,T)$ [not (Ref. 39)] compares similarly to $S^*(T)$ for $t'\neq 0$ as for $t'=0$ (see Fig. 4). The orange (gray) dotted curve is for $t'=0$ to facilitate an easy comparison. As an example of the other sign of t', namely, $t'/t=0.2$, (d) shows the expected reduction in $S^*(T)$ for $U=4|t|$ (similar results obtained for $U=0$ and $U=12|t|$ are not shown). The MH limits are projected onto the $T=5|t|$ plane for finite U [red (gray) line] and infinite U [blue (black) dotted line].

[Fig. 2(c)], for low to intermediate temperatures. As the temperature is continually raised, the condition $|t|\ll U\ll T$ is eventually obtained. The thermopower is then entropy dominated and begins to approach its entropy determined MH limit. This MH limit, of course, is that of the uncorrelated band since an infinite temperature always dominates any effects of finite U interactions. Therefore, one only expects the thermopower of the large U Hubbard model to approach the infinite U MH limit when the condition $|t|\ll T\ll U$ is obtained, which in our calculations is for low to intermediate temperatures. However, we emphasize that for the highest temperature $T=5|t|$, the thermopower remains negative for $n=0.875$ and $U=12|t|$.

In Figs. 3(a)–3(c), we plot the MH term of the thermopower $[S_{MH}(T)]$ versus temperature and filling for $U=0$, $4|t|$, and $12|t|$, respectively. Also shown is $S^*(T)$ for comparison. Interestingly, the transport term increases the low to intermediate temperature thermopower for all fillings in the noninteracting and weakly interacting cases. For the strongly interacting case in Fig. 3(c), the transport term begins to decrease the thermopower at low temperatures and high-fillings ($n\geqslant 0.75$).

The results in this section can be directly compared with Ref. 38 which used the FTL method which allowed rings of up to $\mathcal{L}=14$ sites. Their results were for a much lower window of temperatures $0.2|t|<T<2|t|$ and show a greater thermopower suppression for more modest values of U compared to the present work. The thermopower in the low temperature regime is very sensitive to any changes in either the $S_{tr}(T)$ or $S_{MH}(T)$. Considering that Ref. 38 used a larger system but an approximation, it is unclear as to the nature of the discrepancy between those results and the present study. However, the qualitative behavior of both calculations is consistent.

Next, the full frequency and temperature dependence of the thermopower is investigated. Figures 4(a)–4(h) plot the difference in the full frequency dependent thermopower minus the infinite frequency limit, i.e., $S(\omega,T)-S^*(T)$. For the weak coupling [Figs. 4(a)–4(d)] case, there is little frequency dependence except for when $\omega\sim U$ at low to intermediate temperatures. In what is surely a consequence of the finite sized system, there appears to be an even-odd effect in that for even numbers of electrons [Fig. 4(c) and not shown], $S(\omega,T)-S^*(T)$ is positive for $\omega<U$ and negative for $\omega>U$, while for odd numbers of electrons [Figs. 4(a)–4(d)], the opposite effect is observed. Of course, for half-filling there is no frequency dependence (not shown).

The same qualitative behavior is found for the strongly correlated regime in Figs. 4(e)–4(h). Again the even-odd effect is obtained [cf. Fig. 4(g) vs Figs. 4(e), 4(f), and 4(h)] and the frequency dependence is generally weak except for $\omega\sim U$. The main difference between the $U=12|t|$ and the $U=4|t|$ cases is that the frequency dependence at $\omega\sim U$ in the former is larger. It should be kept in mind that the largest frequency dependences occur for the lowest temperatures and the thermopower for a finite sized system in the low temperature regime is susceptible to finite sized effects that could possibly not survive in the thermodynamic limit.

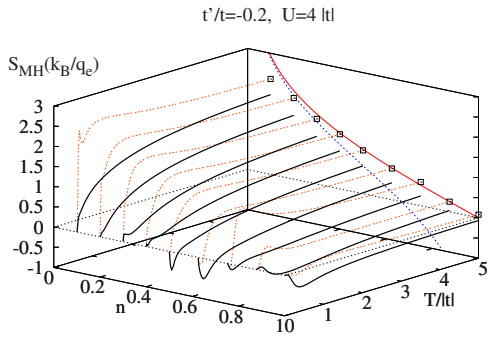

FIG. 6. (Color online) $S_{MH}(T)$ (black line) as a function of filling n and temperature T. The orange (gray) dotted lines are the infinite frequency limit $S^*(T)$ for comparison. Projected onto the $T=5|t|$ plane are the MH limits for both the finite [red (gray) line] and infinite U [blue (black) dotted line] cases.

Therefore, it is safe to assume that our results are qualitatively representative of a thermodynamically large Hubbard model but perhaps not quantitatively accurate.

Similar qualitative frequency dependence was seen in Ref. 38 for a low temperature slice ($T=0.5|t|$) and high fillings ($n>0.7$). The difference between that work and the present work is that the frequency dependence occurred nearer to $\omega \sim U/2$ in the former, whereas in the present result the largest frequency dependence occurs near $\omega \gtrsim U$.

Unless one is concerned with extremely low temperatures and frequencies similar in magnitude to the interaction strength U, the infinite frequency thermopower $S^*(T)$ is a good representative of the full thermopower $S(\omega,T)$. Recently, a similar calculation on the strongly correlated t-J model for a two-dimensional triangular lattice was carried out in Ref. 31, where it was found that the frequency dependence was much weaker, justifying the use of $S^*(T)$ in place of $S(\omega,T)$.

2. *Frustrated thermopower (Hubbard)*

Here, we investigate the effect of frustration on the thermopower by considering the case of a nonzero second-neighbor hopping amplitude $|t'|/t=0.2$.

Shastry[17–19] predicted a low to intermediate temperature enhancement of the thermopower via a high temperature expansion of the high frequency limit $S^*(T)$ for the geometrically frustrated two-dimensional triangular lattice t-J model. In that case, changing the sign of the hopping (making the system electrically frustrated) was found to enhance the thermopower at intermediate temperatures. Haerter *et al.*[6] and Ref. 31 more thoroughly investigated that particular case.

In one dimension, it is similarly expected that an enhancement of the thermopower will occur when a second-neighbor hop is added to the kinetic energy which frustrates the lattice and destroys integrability.

Figures 5(a)–5(d) show $S^*(T)$ versus temperature and filling for the electrically frustrated values of $t'/t=-0.2$ [Figs. 5(a)–5(c)] and $t'/t=0.2$ [Fig. 5(d)]. For this case, we do not plot the full frequency dependence but remark that it is similar qualitatively and quantitatively to the $t'=0$ case.[39]

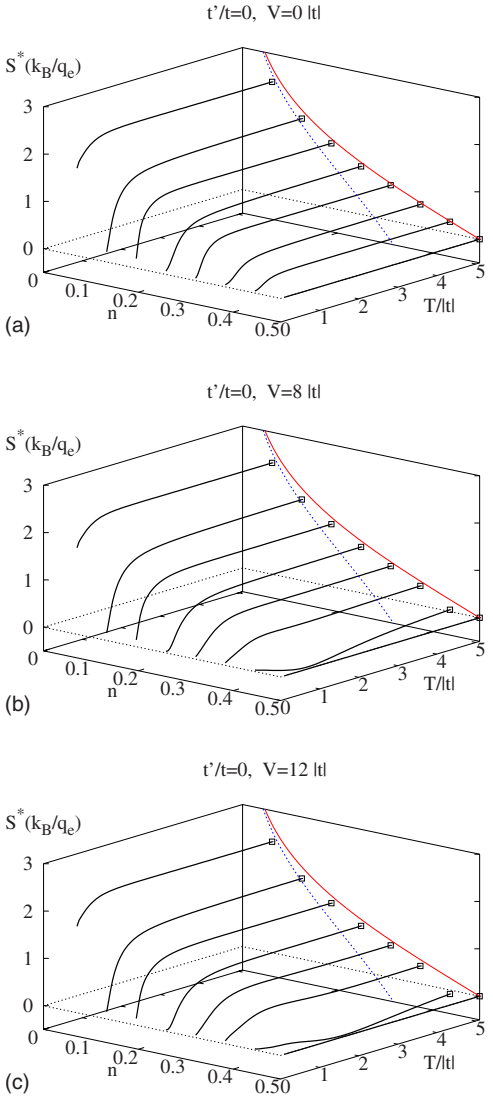

FIG. 7. (Color online) $S^*(T)$ (black line) as a function of filling n and temperature T. Projected onto the $T=5|t|$ plane are the MH limits for both the finite [red (gray) line] and infinite V [blue (black) dotted lines] situations.

When $t>0$ and $t'<0$, the system is electronically frustrated and thermopower is enhanced at low temperatures. The enhancement is seen to arise almost purely from the transport term of the thermopower [first term in Eq. (9)]. Figure 6 shows $S^*(T)$ and the MH term $S_{MH}(T)$ for $t'/t=-0.2$ and $U=4|t|$ as a representative example. Similar to the results displayed in Fig. 3, the low temperature thermopower is dominated by the transport term, and in the case of $t'/t=-0.2$, that domination is even more pronounced as it produces an enhancement peak.

For small fillings, the enhancement has weak U dependence although the noninteracting case seems to be tending to diverge at very low temperatures [$n=0.1$ and $n=0.2$ in Fig. 5(a)], which is most certainly a finite size artifact. In fact, for frustrated $U=0$ case, the thermopower has been calculated exactly for the thermodynamically large system by computing (numerically) the necessary Fermi-Dirac integrals and no such divergent tendency was obtained at any tem-

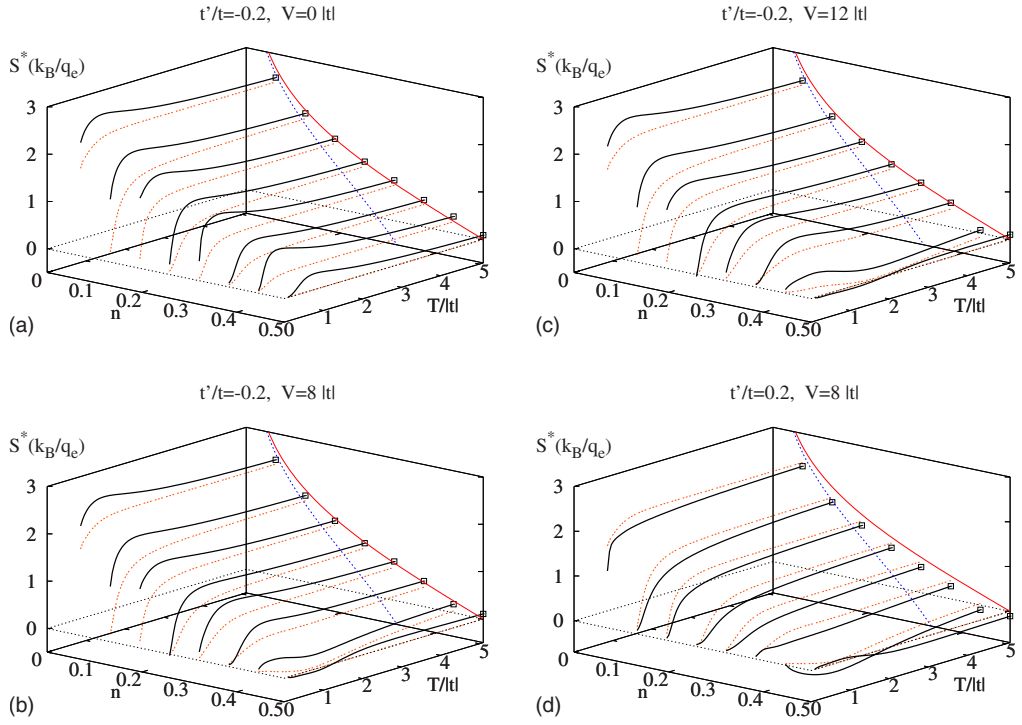

FIG. 8. (Color online) $S^*(T)$ as a function of filling n and temperature T for (a) $V=0$, (b) $V=8|t|$, and (c) $V=12|t|$. The full $S(\omega,T)$ compares similarly to $S^*(T)$ as for the $t'=0$ case (see Fig. 4). The orange (gray) curve is $S^*(T)$ for $t'=0$ to facilitate an easy comparison. As an example of the other sign of t', namely, $t'/t=0.2$, (d) shows the expected reduction in $S^*(T)$ for $V=8|t|$. The MH limits are projected onto the $T=5|t|$ plane for finite V [red (gray) line] and infinite V [blue (black) dotted line].

perature or density. At fillings above $n=0.5$, there are interaction effects which are visible at low temperatures. For the frustrated case discussed here, the thermopower still mostly achieves its MH limit by $T=5|t|$ as expected.

For the situation when t and t' are both positive, there is a suppression of the thermopower at low temperatures [see Fig. 5(d)], hence the opposite effect. Only the weakly correlated $U=4|t|$ case is plotted to illustrate this.

For both signs of t' at half-filling ($n=1$), the thermopower is no longer identically zero since the addition of a nonzero t' destroys the particle-hole symmetry; however, the thermopower remains quite small at this density.

B. t-V model

Most of the considerations of the thermopower for the Hubbard model also apply to the t-V model. In particular, this model too has particle-hole symmetry at half-filling ($n=0.5$ instead of $n=1$ as for the Hubbard model, since the spin degree of freedom is absent) and thus the thermopower is identically zero at all temperatures. The thermopower is once again divergent in the band-insulator limits ($n=0$ and $n=1$) and also in the vicinity of the Mott insulator ($n=0.5$) in the presence of strong correlations (large V). In the high temperature limit ($k_BT \gg t$), the thermopower is pinned by the entropy as in the Hubbard model. The MH limit can be calculated in a straightforward manner in the $V=0$ and $V=\infty$ regimes from the expressions already derived for the extended Hubbard model (on-site U and nearest-neighbor V).[34]

The t-V model corresponds to setting $U=\infty$ and removing the spin degeneracy. We thus obtain

$$\lim_{T\to\infty} S_{MH}(T) = \begin{cases} \dfrac{k_B}{q_e} \ln\left(\dfrac{1-n}{n}\right) & \text{(i)} \\ \dfrac{k_B}{q_e} \ln\left(\dfrac{(1-2n)^2}{n(1-n)}\right) & \text{(ii)}, \end{cases} \tag{11}$$

where Eq. (11)(i) corresponds to finite V and $0 \leqslant n \leqslant 1$, while Eq. (11)(ii) corresponds to infinite V and $0 \leqslant n \leqslant 0.5$. As mentioned previously, the expressions in Eq. (11) were first considered in Ref. 34 with the second line (the infinite V limit) being the third equation of Table 1 in Ref. 34 with the spin degeneracy removed.

An important distinction between the Hubbard model and the t-V model is that the energy current operator commutes with the Hamiltonian in the latter. From the Kubo formula, this implies that in Eq. (9), $S_{tr}(\omega,T)=0$ for all $\omega \neq 0$ and $S(\omega,T)=S_{MH}(T)$ for all $\omega \neq 0$. Since $S^*(T)=S(\omega\to\infty,T)$, this leads to $S^*(T)=S_{MH}(T)$ at all temperatures and fillings in this model. From Eq. (6), we have that $\langle\hat{\Phi}_{xx}\rangle=-\mu\langle\hat{\tau}_{xx}\rangle$, a fact that has been verified numerically. A further consequence is that $\kappa(\omega,T)/T\sigma(\omega,T)=S(\omega,T)^2$ for all $\omega \neq 0$ and consequently $L(\omega>0,T)=0$, implying $Z(\omega>0,T)T=\infty$ in this system. Physically, the energy current commuting with the Hamiltonian means that the system is unable to transport any heat at finite frequency in the presence of a temperature or potential gradient without transporting charge. In zero current conditions, where there is no charge transport, there is no heat

transport as well and the thermal conductivity is zero. This causes the Lorenz number to be zero and the FOM to be infinite. All the above considerations rely on the fact that the energy current commutes with the Hamiltonian. This is no longer true with $t' \neq 0$ and all the quantities mentioned above will have nonzero values at $\omega \neq 0$.

1. Unfrustrated thermopower (t-V)

The behavior of the thermopower for the t-V model is quite similar to that of the Hubbard model even though the thermopower has no transport term for $t'=0$ and is, therefore, simply $S_{MH}(T)$. Plotted in Figs. 7(a)–7(c) is the thermopower $S^*(T)$ for three values of the interaction strength, $V=0$, $V=8|t|$, and $V=12|t|$. At low densities, the thermopower very rapidly rises to nearly its full MH limit by $T \approx 2|t|$. The initial (mostly) linear slope is reduced as the filling is increased. The effects of interactions are not readily seen until the somewhat large filling of $n=0.4375$, where the thermopower is markedly reduced for all temperatures shown. Eventually, as the temperature is raised, the interaction effects are washed out as the thermopower approaches its MH limit.

Compared to the Hubbard model, however, the interaction effects appear weaker (perhaps due to the absence of the transport term) and affect only the highest fillings studied (other than the half-filled case $n=0.5$ which is pinned at zero due to particle-hole symmetry).

2. Frustrated thermopower (t-V)

Adding a second-neighbor t' hopping term has an effect very similar to the one in the Hubbard model, again destroying the integrability and the particle-hole symmetry of the model. A result of the latter is that the thermopower is no longer identically zero at half-filling. As in the Hubbard model, a more interesting aspect of introducing a second-neighbor hopping is that it produces frustration depending on its sign.

The thermopower is plotted as a function of temperature and filling for $V=0$, $V=8|t|$, and $V=12|t|$ for the case of $t'/t=-0.2$ in Figs. 8(a)–8(c) and for $V=8|t|$ for the case of $t'/t=0.2$ in Fig. 8.

A positive sign of t' reduces the value of $S^*(T)$ compared to $t'=0$, while a negative sign enhances it. $S^*(T)$ starts out being zero at $T=0$ and approaches the Mott-Heikes limit as $T \to \infty$ independent of the value of t'. Since $S^*(T)$ for $t'=0$ is a monotonically increasing function of T, it stands to reason that $S^*(T)$ reaches a maximum at some value of T for $t' < 0$ and decreases toward the Mott-Heikes limit. This is indeed what is seen in our calculations, as demonstrated in Fig. 8, similar to the situation of the Hubbard model. This is very interesting since it affords the possibility of thermopower enhancement through frustration.

Even though we do not explicitly calculate $S(\omega,T)$ for the t-V model when $t' \neq 0$, we comment that the introduction of t' causes the energy current operator not to commute with the Hamiltonian. Consequently, $S(\omega,T)$ is now no longer independent of ω and approaches $S^*(T)$ as $\omega \to \infty$ as in the Hubbard model. Presumably, the full frequency dependence

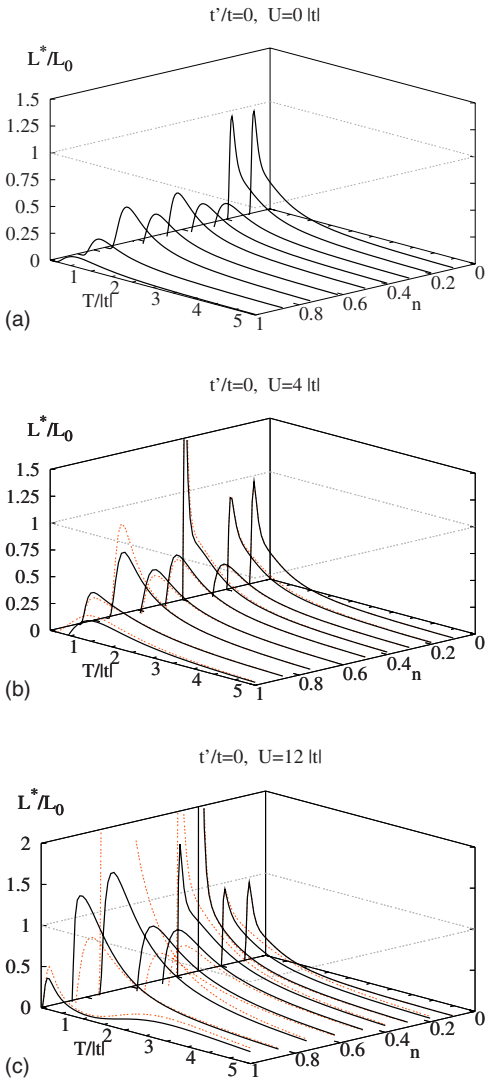

FIG. 9. (Color online) $L^*(T)/L_0$ as a function of filling n and temperature T (black line). The orange (gray) dotted line is the dc limit $L(0,T)$ for comparison. Note that for $U=0$ (a), there is no frequency dependence of $L(\omega,T)$ and $L^*(T)=L(0,T)$. The full $L(\omega,T)$ (not shown) compares similarly to the frequency dependence of the thermopower for $U=4|t|$ and $12|t|$ in Fig. 4.

is similar to that seen in the Hubbard model but has not been calculated explicitly.

Although not shown for the t-V model, we point out that similar to the Hubbard model, the thermopower enhancement peak arises from the transport term of the thermopower almost exclusively as discussed in Sec. IV A 2 and shown in Fig. 6.

V. LORENZ NUMBER

The Lorenz number [Eq. (4)] is an important quantity as it measures the ratio of the thermal to the electrical conductivity. Further, it is a key ingredient to the FOM (containing both the thermopower and Lorenz number) which measures the efficiency of a thermoelectric material. Note that there is usually a contribution to the Lorenz number coming from

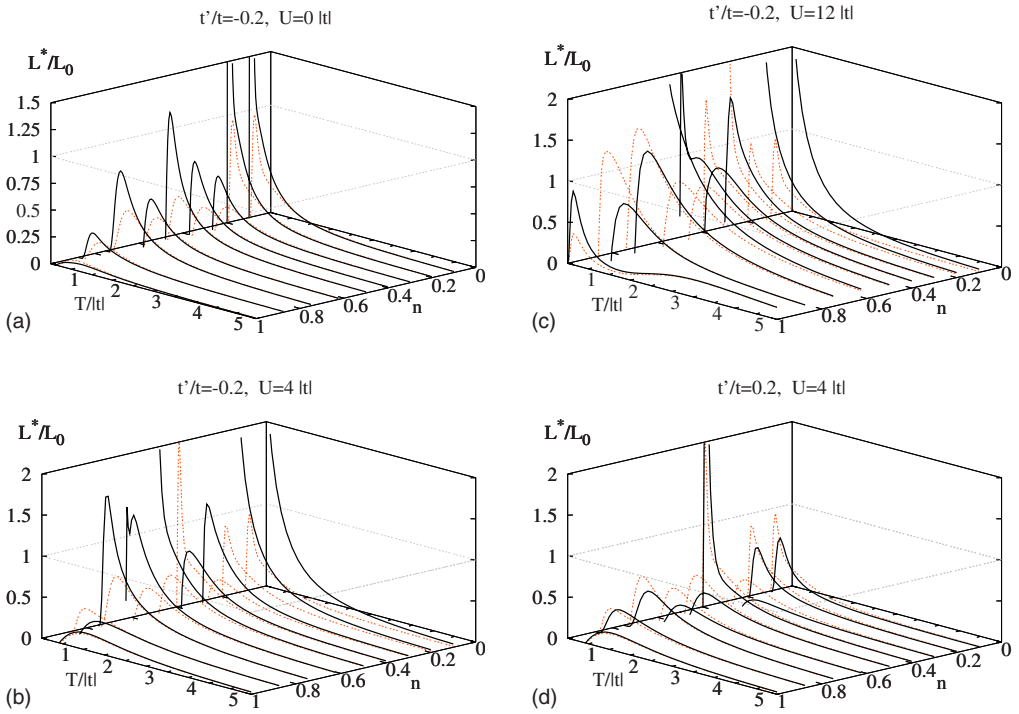

FIG. 10. (Color online) $L^*(T)/L_0$ as a function of filling n and temperature T for (a) $U=0$, (b) $U=4|t|$, and (c) $U=12|t|$. The full $L(\omega,T)$ compares similarly to frequency dependence of the thermopower. The orange (gray) dotted curve is the $t'=0$ case to facilitate an easy comparison. (d) is an example of the other sign of t', namely, $t'/t=0.2$.

lattice vibrations (phonons). In this work, however, we only consider the electronic contributions to the Lorenz number.

As noted in Ref. 31, the chemical potential is absent from Eq. (4) and the Lorenz number can be understood completely within the canonical ensemble. Evidently, it is determined through electron transport alone. At zero temperature, it is well known that the Lorenz number is equal to the constant $L_0=(\pi k_B/\sqrt{3}q_e)^2$ which is just the Wiedemann-Franz law.[32,40]

As discussed in Ref. 31, for noninteracting systems, the limit $\lim_{T\to 0}L(\omega,T)=L_0$ comes from two effects. Similar to the thermopower, we attempt to limit the finite sized system induced divergences of the Lorenz number by forcing the subtle balances necessary to ensure a finite Lorenz number as $T\to 0$. The exact method used here is the same as in Ref. 31 and not repeated. Ultimately, we are able to control the divergences to a large degree; however, we are unable to answer the very interesting question of whether the value of L_0 is a universal constant independent of electron interactions.

Below, we present $L^*(T)$ as a function of temperature and filling. The frequency dependence of $L(\omega,T)$ (not shown here) is comparable to $S(\omega,T)$ in that it is generally weak with a feature near $\omega=U$.

A. Unfrustrated Lorenz number (Hubbard)

Figures 9(a)–9(c) show the "normalized" high frequency Lorenz number $L^*(T)/L_0$ as a function of temperature and filling for the noninteracting, the weakly coupled, and the strongly coupled situations for the case of $t'=0$. In Figs. 9(b) and 9(c), the dc limit of the full frequency dependent Lorenz number is also plotted, i.e., $L(0,T)/L_0$.

For the noninteracting case [Fig. 9(a)], $L^*(T)$ is suppressed at low temperatures as the filling increases toward half-filling. For a thermodynamically large system, the Lorenz number starts at L_0 and quickly decreases as a function of temperature, similar to what is shown here. In the weakly coupled regime [Fig. 9(b)], $L^*(T)$ is very similar to the noninteracting case for fillings below approximately $n=0.4$. For $n\geqslant 0.5$, however, it is enhanced at low temperatures. The dc limit is quite similar to the infinite frequency limit showing the usefulness and accuracy of $L^*(T)$ in the weakly coupled regime. When the interactions are strong [Fig. 9(c)], there is a much stronger enhancement of $L^*(T)$ for $n\geqslant 0.3$ and the enhancement persists to higher temperatures. The dc limit in this case is not as similar to $L^*(T)$ as it is for the weakly coupled regime.

B. Frustrated Lorenz number (Hubbard)

For nonzero t', we plot $L^*(T)/L_0$ as a function of filling and temperature along with $L^*(T)/L_0$ for the $t'=0$ to ease comparison in Figs. 10(a)–10(d).

For the electronically frustrated scenario ($t'<0$), the Lorenz number in Figs. 10(a)–10(c) is also enhanced compared to the unfrustrated ($t'=0$) situation at low temperatures. This enhancement is also more pronounced for low than for high fillings and increases with increasing interaction strength U, especially close to half-filling.

When $t'>0$ in the weakly coupled regime [Fig. 10(d)], the Lorenz number is very slightly suppressed compared to

the $t'=0$ situation as one would expect from the $t'<0$ results and the previous investigation of the thermopower.

Generally, for both $t'=0$ and $t'\neq 0$, the Lorenz number is appreciably below L_0 for all temperatures above approximately $T\sim 1.5|t|$.

VI. FIGURE OF MERIT

The figure of merit is the number that is most important when it comes to technological applications regarding thermoelectrics, as mentioned above, being a measure of thermoelectrical efficiency. In our calculations, we are ignoring the lattice contribution to the Lorenz number so our FOM calculated is that due to electronic contributions only.

Using the "tricks" to handle finite size effects for $S^*(T)$ and $L^*(T)$ (see Ref. 31), we calculate the high frequency expansion of the FOM $[Z^*(T)T]$ given in Eq. (8).

A large FOM can arise in essentially two ways. One way is for the thermopower, which is squared in the numerator, to be large. The other is for the Lorenz number in the denominator to be small. The Lorenz number has been shown in Sec. V to tend to zero as the temperature tends to infinity. The thermopower, on the other hand, reaches a constant, and finite, MH limit as $T\to\infty$. Hence, the electronic contribution to the FOM will eventually grow to infinity as the temperature is increased without bound.

In the following sections, we plot $Z(\omega,T)T$ as a function of T and filling n.

A. Unfrustrated figure of merit (Hubbard)

Figures 11(a)–11(c) show the FOM for the unfrustrated $(t'=0)$ Hubbard model for the noninteracting case, the weakly coupled case, and the strongly coupled case. Also plotted is the dc limit of the full frequency dependent FOM. In the noninteracting case [Fig. 11(a)], the FOM grows apparently quadratically in temperature with a coefficient that decreases inversely with filling. This behavior is seen in the weakly coupled and strongly coupled cases as well [see Figs. 11(b) and 11(c)], although the FOM is decreased more for lower fillings.

The full frequency behavior of the FOM (not shown) is very similar to the high frequency limit, evidently because the differences in the two limits for the thermopower and Lorenz number largely cancel one another out.

B. Frustrated figure of merit (Hubbard)

In Figs. 12(a)–12(d), we investigate the effects of frustration on the FOM for the $t'<0$ and $t'>0$ cases, respectively.

For the electronically frustrated system $(t'<0)$, the FOM is suppressed compared to $t'=0$ except for the noninteracting case where they are very similar. The larger interaction strength has the effect of further suppressing the FOM especially for low fillings.

Alternatively, the case of $t'>0$ that produced suppression in both $S^*(T)$ and $L^*(T)$ has a very slight enhancement in the FOM shown in Fig. 12(d). This nicely illustrates the complicated way in which the thermopower and Lorenz number combine to produce the FOM.

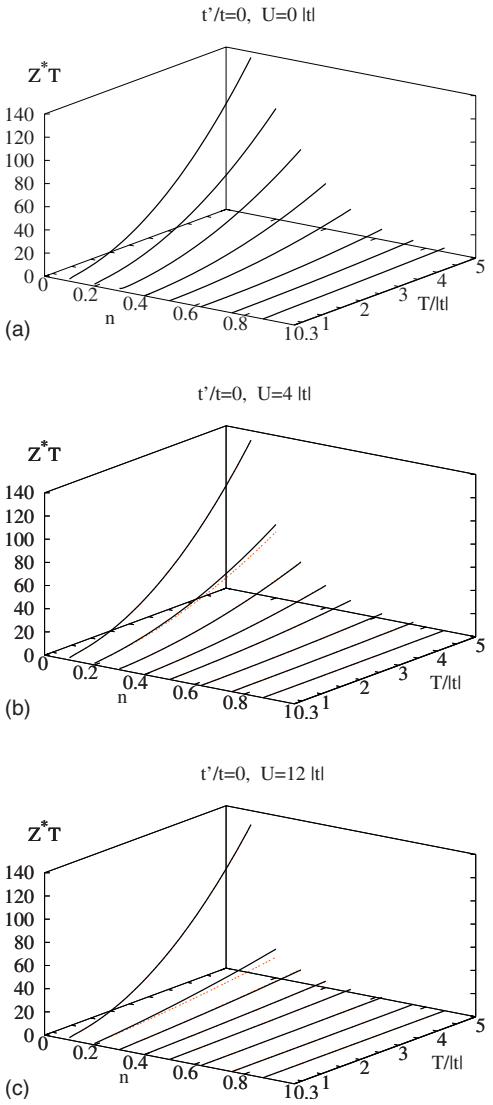

FIG. 11. (Color online) $Z^*(T)T$ as a function of filling n and temperature T as the solid black line for (a) $U=0$, (b) $U=4|t|$, and (c) $U=12|t|$. The orange (gray) dotted curve is the dc limit of the full $Z(\omega,T)T$ for comparison, i.e., $Z(0,T)T$. Note that for $U=0$ (a), there is no frequency dependence.

VII. CONCLUSION

In this paper, we have computed thermoelectrical properties of the Hubbard model and the spinless fermion t-V model on one-dimensional rings investigating, in particular, the thermopower (Hubbard and t-V), Lorenz number, and figure of merit (Hubbard only). Our calculations are detailed calculations of these thermoelectric variables for strongly correlated models in that they consider the full range of model parameter space. By adding a second-neighbor hopping term with amplitude t', both positive and negative, we were able to destroy the integrability of these models and induce frustration. The electronically frustrated $(t'<0)$ Hubbard and t-V models displayed an enhanced thermopower at low to intermediate temperatures. For the Hubbard model, the Lorenz number was also found to have low temperature

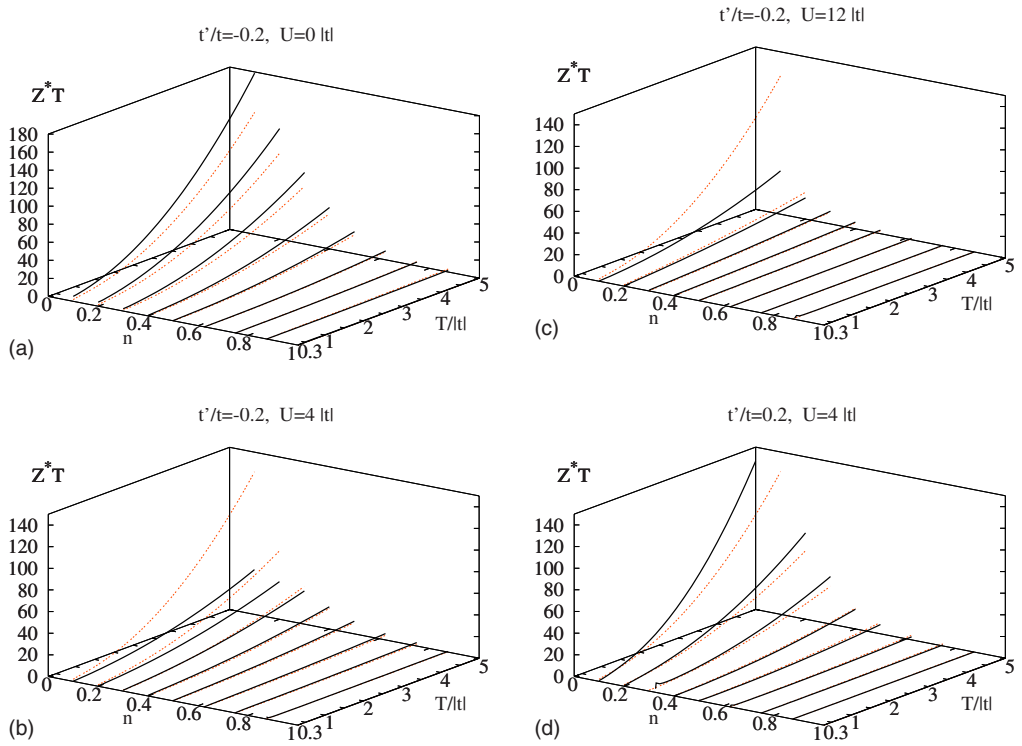

FIG. 12. (Color online) $Z^*(T)T$ as a function of filling n and temperature T for (a) $U=0$, (b) $U=4|t|$, and (c) $U=12|t|$. The full frequency dependent $Z(\omega,T)T$ compares similarly to the frequency dependence of the thermopower. The orange (gray) dotted curve is for $t'=0$ to facilitate an easy comparison. For an example of the other sign of t', we plot the situation $t'/t=0.2$ in (d).

enhancements. However, the FOM did not produce the same enhancement but instead a suppression for nonzero interaction strength U. Nevertheless, the FOM was modestly enhanced by the opposite sign of hopping $t'>0$ at low fillings.

For the Hubbard model, the thermopower had a generally weak frequency dependence other than a sometimes large feature near $\omega \sim U$. This behavior was also obtained, but not shown here, for the Lorenz number and FOM. This has the consequence that the high frequency versions of the thermopower, Lorenz number, and FOM recently proposed by Shastry[17–19] provide a good approximation to the full dynamical quantities for most values of the system parameters.

ACKNOWLEDGMENTS

We gratefully acknowledge support from Grant No. NSF-DMR0408247 and DOE-BES Grant No. DE-FG02-06ER46319. We acknowledge helpful conversations with J. E. Moore. S.M. thanks the DOE for support.

*peterson@physics.ucsc.edu

[1] Y. Tokura, Phys. Today **56**(7), 50 (2003).
[2] M. Imada, A. Fujimori, and Y. Tokura, Rev. Mod. Phys. **70**, 1039 (1998).
[3] B. G. Levi, Phys. Today **56**(8), 15 (2003).
[4] I. Terasaki, Y. Sasago, and K. Uchinokura, Phys. Rev. B **56**, R12685 (1997).
[5] Y. Y. Wang, N. S. Rogado, R. J. Cava, and N. P. Ong, Nature (London) **423**, 425 (2003).
[6] J. O. Haerter, M. R. Peterson, and B. S. Shastry, Phys. Rev. Lett. **97**, 226402 (2006).
[7] J. Hone, I. Ellwood, M. Muno, A. Mizel, M. L. Cohen, A. Zettl, A. G. Rinzler, and R. E. Smalley, Phys. Rev. Lett. **80**, 1042 (1998).
[8] F. Zhou, J. H. Seol, A. L. Moore, L. Shi, Q. L. Ye, and R. Scheffler, J. Phys.: Condens. Matter **18**, 9651 (2006).
[9] A. J. Epstein, J. S. Miller, and P. M. Chaikin, Phys. Rev. Lett. **43**, 1178 (1979).
[10] J. F. Kwak, G. Beni, and P. M. Chaikin, Phys. Rev. B **13**, 641 (1976).
[11] A. P. Ramirez, in *More Is Different*, edited by N. P. Ong and R. N. Bhatt (Princeton University Press, Princeton, NJ, 2001), p. 255.
[12] J. O. Haerter and B. S. Shastry, Phys. Rev. Lett. **95**, 087202 (2005).
[13] C. L. Kane and M. P. A. Fisher, Phys. Rev. Lett. **76**, 3192 (1996).
[14] B. S. Shastry, Phys. Rev. Lett. **56**, 2453 (1986).
[15] C. N. Yang and C. P. Yang, Phys. Rev. **150**, 321 (1966).
[16] B. Sutherland, *Beautiful Models* (World Scientific, Singapore, 2004).
[17] B. S. Shastry, Phys. Rev. B **73**, 085117 (2006); http://

physics.ucsc.edu/~sriram/papers_all/ksumrule_errors_etc/evolving.pdf
[18] B. S. Shastry, Phys. Rev. B **74**, 039901(E) (2006).
[19] B. S. Shastry (unpublished).
[20] R. Kubo, J. Phys. Soc. Jpn. **12**, 570 (1957).
[21] G. Kotliar and D. Vollhardt, Phys. Today **63**(3), 53 (2004).
[22] A. Georges, G. Kotliar, W. Krauth, and M. J. Rozenberg, Rev. Mod. Phys. **68**, 13 (1996).
[23] J. Jaklic and P. Prelovsek, Adv. Phys. **49**, 1 (2000).
[24] T. Maier, M. Jarrell, T. Pruschke, and M. H. Hettler, Rev. Mod. Phys. **77**, 1027 (2005).
[25] V. S. Oudovenko and G. Kotliar, Phys. Rev. B **65**, 075102 (2002).
[26] G. Pálsson and G. Kotliar, Phys. Rev. Lett. **80**, 4775 (1998).
[27] The t-V model is limited for our purposes partly due to the fact that some of the transport coefficients turn out to be identically zero in this model as discussed in Sec. IV B and partly because the calculation of some of the operators is very involved, owing to the interaction being between neighboring sites compared to the on-site Hubbard interaction.
[28] The computational limitations for the Hubbard model are due mostly to the double sum over states when calculating conductivities via the Kubo formulas rather than due to the diagonalization proper.
[29] C. Gros, K. Hamacher, and W. Wenzel, Europhys. Lett. **69**, 616 (2005).
[30] G. D. Mahan, *Many-particle Physics* (Plenum, New York, 1990).
[31] M. R. Peterson, B. S. Shastry, and J. O. Haerter, arXiv:0705.3867v1 (unpublished).
[32] J. M. Ziman, *Principles of the Theory of Solids* (Cambridge University Press, Cambridge, 1979).
[33] The mean energy level spacing is also very insensitive to the value of t' used here.
[34] P. M. Chaikin and G. Beni, Phys. Rev. B **13**, 647 (1976).
[35] C. A. Stafford, Phys. Rev. B **48**, 8430 (1993).
[36] E. H. Lieb and F. Y. Wu, Phys. Rev. Lett. **20**, 1445 (1968).
[37] The MH limit for a finite system does not exactly equal the MH limit for the infinite system even in the $T \to \infty$ limit due to the finite nature of the Hilbert space.
[38] M. M. Zemljic and P. Prelovsek, Phys. Rev. B **71**, 085110 (2005).
[39] For the frustrated case, there is a frequency dependence at half-filling, unlike the unfrustrated case, arising from the broken particle-hole symmetry.
[40] N. W. Ashcroft and D. N. Mermin, *Solid State Physics* (Brooks-Cole, Belmont, MA, 1976).